Journal of Biomechanics 95 (2019) 109304

Contents lists available at ScienceDirect

Journal of Biomechanics

journal homepage: www.elsevier.com/locate/jbiomech
www.JBiomech.com

Compressive fatigue and endurance of juvenile bovine articular cartilage explants

Paul E. Riemenschneider, Melanie D. Rose, Martina Giordani, Sean M. McNary *

Department of Orthopaedic Surgery, School of Medicine, University of California, Davis, Sacramento, CA, USA

ARTICLE INFO

Article history:
Accepted 31 July 2019

Keywords:
Articular cartilage
Fatigue
Endurance
Cyclic loading
Durability

ABSTRACT

Articular cartilage is an enduring tissue. For most individuals, articular cartilage facilitates a lifetime of pain-free ambulation, supporting millions of loading cycles from activities of daily living. Although early studies into osteoarthritis focused on the role of mechanical fatigue in articular cartilage degeneration, much is still unknown regarding its strength and endurance characteristics. The compressive strength of juvenile, bovine articular cartilage explants was determined to be loading rate-dependent, reaching a maximum strength of 29.5 ± 4.8 MPa at a strain rate of 0.10 %/sec. The fatigue and endurance properties of articular cartilage were characterized utilizing a material testing system, as well as a custom, validated instrument termed the two degrees-of-freedom endurance meter (endurometer). These instruments characterized fatigue in articular cartilage explants at loading levels ranging from 10 to 80 % strength (%*S*), up to 100,000 cycles. Cartilage explants displayed characteristics of fatigue – fatigue life increased as the loading magnitude decreased. All explants failed within 14,000 cycles at loading levels between 50 and 80 %*S*. At 10 and 20 %*S*, all explants endured 100,000 loading cycles. There was no significant difference in equilibrium compressive modulus between run-out explants and unloaded controls, although the pooled modulus increased in response to testing. Histological staining and biochemical assays revealed no material changes in collagen, sulfated glycosaminoglycan, or hydration content between unloaded controls and explants cyclically loaded to run-out. These results suggest articular cartilage may have a putative endurance limit of 20 %*S* (5.86 MPa), with implications for articular cartilage biomechanics and mechanobiology.

1. Introduction

Articular cartilage plays a crucial role in human locomotion, lining the articulating surfaces of long bones and distributing loads while maintaining low friction and wear properties (McNary et al., 2012). This tissue must endure millions of cycles of loading generated by activities of daily living (ADL) such as walking and stair climbing that can reach compressive stresses up to 18 MPa (Hodge et al., 1986). For example, adults over the age of 50 years have been observed to take between 2,000 and 9,000 steps per day (Tudor-Locke et al., 2009), which extrapolates to over 1.6 million loading cycles per year. For the segment of the population unaffected by arthritis, healthy articular cartilage is an enduring tissue capable of supporting over 100 million loading cycles over a lifetime.

Repetitive loading can result in alterations to the mechanical properties of a material, a process known as mechanical fatigue (Suresh, 1998). These repetitive stresses from cyclic loading generate microstructural damage. Accumulation and progression of microscopic defects can lead to complete failure or breakage of a material at stresses below its ultimate strength. The fatigue properties of materials are traditionally characterized via total fatigue life where a material is cyclically loaded to failure at various fractions of its ultimate strength. These results are plotted as stress amplitude in relation to cycles to failure, or S-N curves. S-N curves typically plateau at greater than 10^6–10^7 cycles, a region defined as the fatigue or endurance limit. The endurance limit denotes the stress amplitude a defect-free material can theoretically support for an infinite number of cycles (Suresh, 1998). Despite its reputation as a durable tissue when healthy, the endurance properties of articular cartilage are unknown.

Articular cartilage fatigue was first studied in the 1970s, motivated by the hypothesis that surface fibrillation in osteoarthritis (OA) arose from mechanical fatigue. Weightman et al. (1973) cyclically indented articular cartilage and observed surface fibrillation.

* Corresponding author at: Department of Orthopaedic Surgery, School of Medicine, University of California, Davis, Research Building I, Room 2000, Sacramento, CA 95817.
E-mail address: smmcnary@ucdavis.edu (S.M. McNary).

https://doi.org/10.1016/j.jbiomech.2019.07.048
0021-9290/

The authors proceeded to study the fatigue properties of cartilage loaded under tension and observed classical fatigue behavior (Weightman et al., 1978). In subsequent years, cartilage fatigue from shear (Simon et al., 1989), tension (Bellucci and Seedhom, 2002), and bending (Sadeghi et al., 2017) have been studied. In addition to modality, loading frequency is an important determinant of articular cartilage damage and a factor in fatigue. Crack growth in articular cartilage increases as loading frequency increases under both compressive and tensile loading (Sadeghi et al., 2015, 2018). While articular cartilage experiences complex strain fields, including tension and shear during physiological loading, the applicability of these results are limited as the native tissue is predominantly loaded in compression (Canal et al., 2008; Chan et al., 2016). Mechanical fatigue from compressive loading has been studied (Kaplan et al., 2017; McCormack and Mansour, 1998), but fundamental mechanical characteristics of articular cartilage such as the fatigue life and endurance limit remain unknown.

Our understanding of OA has progressed from a "wear and tear" paradigm, to a multifactorial etiology that includes elements such as traumatic joint injury, age, genetic predisposition, and mechanical overloading from obesity or anatomical malformation (Felson, 2013; Sandell, 2012). Cyclic loading of living joints in animal models have been studied over the years to elucidate the interactions between repetitive loading and synovial joint homeostasis. Radin and colleagues investigated the effects of cyclic compressive loading in rabbits and guinea pigs, and reported an increase in subchondral bone stiffness prior to fibrillation and further cartilage degeneration (Radin et al., 1984; Simon et al., 1972). Other studies have examined long-term joint loading *in vivo* through treadmill exercise and non-invasive tibial loading (Ko et al., 2013; Lapvetelainen et al., 1995; Poulet et al., 2011). To better understand the connection between repetitive mechanical loading and articular cartilage degeneration, elucidation of the effects of cyclic loading on the biomechanical properties (e.g. fatigue) of the extracellular matrix (ECM) is required.

The principal objective of this study was to characterize articular cartilage fatigue and endurance under compressive loading. For this initial study, 5 mm diameter articular cartilage explants from juvenile, bovine stifle joints were examined as it is a well characterized model tissue with flat and intact articulating surfaces (Mow et al., 1989; Park et al., 2003; Neu et al., 2007). The compressive strength of articular cartilage was measured as a function of strain rate, and then cyclically loaded until failure at fractional levels of this strength. We hypothesized that articular cartilage exhibits fatigue behavior under cyclic, compressive loading. Secondarily, we hypothesized that articular cartilage would display an incipient endurance limit, demarcated *a priori* at 100,000 cycles.

2. Methods

2.1. Tissue acquisition

Articular cartilage explants (5 mm dia.) were obtained from the medial femoral condyle of calf stifle joints (Research 87, Boylston, MA) using a coring reamer (Neu et al., 2007). Explants were washed and trimmed to a uniform thickness of 4 mm containing the superficial, middle, and deep zones using a custom jig. Tissues were wrapped in gauze moistened with phosphate buffered saline (PBS, Affymetrix) and stored frozen (-80 °C). All PBS solutions were supplemented with protease inhibitors prior to use. Prior to testing, the explants were thawed in PBS for one hour at room temperature. Previous studies have shown that a freeze-thaw cycle has a negligible impact on the mechanical properties of articular cartilage explants (Athanasiou et al., 1991; Szarko et al., 2010).

2.2. Compressive strength testing

A set of four explants was obtained from both the load bearing and non-loading bearing regions of the medial femoral condyle (Neu et al., 2007). Both sets (four load bearing explants and four non-load bearing explants) were obtained from the stifle joints of 8 different animals, for a total of 64 specimens. Explant thickness was assessed utilizing contact-sensitive calipers (Mitutoyo, Series 573) before attachment to the bath with 1 μL cyanoacrylate glue and submersion in PBS. Following a 0.2 N tare load, explants were compressively loaded (MTS 858) using a flat, stainless steel platen (12.6 mm dia.) at strain rates of 0.05, 0.1, 1, and 10 %/sec. Compressive failure was defined as the maximum stress preceding a $\geq$10% decrease in load support, which was empirically verified to correspond with compressive failure of articular cartilage.

2.3. Endurance testing of articular cartilage explants

Articular cartilage endurance was characterized at 10–80 %*S* using the endurometer (Supplementary Material, Fig. S1A, Table S1), and MTS 858 for loads exceeding 39 %*S* (Table 1). Explants were obtained from two lots of eight bovine stifle joints, paired by joint. Following measurement of thickness and wet weight, explants were secured to the system with 1 μL cyanoacrylate glue and submerged in a covered, PBS bath. A 0.5 N tare load was applied, followed by a 2.5 N creep load for one hour to measure the unconfined, equilibrium compressive (e.g. Young's) modulus, which was computed as the creep stress normalized to the equilibrium strain (Mauck et al., 2000). Explants were cyclically loaded utilizing a sinusoidal waveform at 1 Hz to failure, or a run-out of 100,000 cycles.

Failure was defined as disruption of the bulk tissue. Bulk tissue disruption (Fig. 4) was empirically determined to correspond with an abrupt increase in peak cyclic strain, resulting in a sigmoidal displacement curve (Fig. 2B). This sigmoidal characteristic (Fig. 2B arrow) was determined via an algorithm that detected the two inflection points in the peak displacement data using the first and second derivatives calculated from backward finite difference approximations (Chapra and Canale, 2015). Failure was also detected via exceeding a load limit of 110% since fatigue-induced changes in cartilage biomaterial properties could cause the proportional-integral-derivative (PID) controller to overload an explant. Cartilage failure was visually verified at the conclusion of every test. In the event run-out occurred, the specimen recovered for three hours at 0.3 N followed by measurement of the post-loading equilibrium modulus. Explant thickness, wet weight, and gross morphology were recorded at least eight hours after loading.

2.4. Histology and biochemical analysis

Explants were fixed in Bouin's solution (Sigma), embedded in paraffin, sectioned (6 μm thick), and mounted on positively charged glass slides. Sections were deparaffinized using xylene and rehydrated with graded ethanol. Toluidine blue and picrosirius red staining were performed using standard techniques (Peng et al., 2014, 2015). For biochemical analysis, run-out explants were lyophilized for 48 h and dry weight measured. The lyophilized tissue was digested in 3.875 U/mL papain (Sigma) in phosphate buffer (pH 7.0) containing 5 mM N-acetyl-L-cysteine and 5 mM EDTA (Sigma) for 18 h at 60 °C. Sulfated glycosaminoglycan (sGAG) content was quantified by a 1,9-dimethylmethylene blue binding assay according to the manufacturer's directions (Biocolor, Blyscan). Total collagen content was quantified using a hydroxyproline assay (Cissell et al., 2017).

Table 1
Endurance testing parameters per loading level.

Explant Set	% Strength (%S)	Max Stress (MPa)	Min Stress (MPa)	Testing System
Group 1	10	3.0	0.13	Endurometer
	20	5.9	0.19	Endurometer
	30	8.9	0.25	Endurometer
	39	11.5	0.32	Endurometer
	39	11.5	0.32	MTS
Group 2	50	14.8	0.38	MTS
	60	17.8	0.45	MTS
	70	20.6	0.51	MTS
	80	23.7	0.57	MTS

2.5. Statistical analysis

A two-way ANOVA (SAS, JMP 13; Factors: strain rate and topographic region), with Tukey's *post hoc* test, was used to assess the compressive strength results. For multiple groupwise comparisons within a single factor, a one-way ANOVA with Tukey's *post hoc* test was employed. Groups not connected by the same letter were determined to be significantly different. For comparisons of two groups, a two-tailed Student's *t*-test was performed (Microsoft Excel). Fatigue life results were log transformed and fit to a linear regression curve. P-values <0.05 were considered statistically significant. All values are presented as mean ± standard deviation.

3. Results

3.1. Compressive strength

The compressive strength of articular cartilage is strain-rate dependent (Fig. 1A and B). Cartilage explants loaded at a strain rate of 1 %/sec exhibited the lowest strength at 22.3 ± 3.9 MPa, while the slowest loading rates of 0.05 and 0.1 %/sec elicited the greatest compressive strength values of 26.9 ± 4.3 and 29.5 ± 4.8 MPa respectively ($p < 0.05$). Failure strain exhibited strain-rate dependence as it significantly increased ($p < 0.03$) with decreasing strain rate, ranging from 42.5 ± 3.5 % at 10 %/sec to 69.8 ± 1.8% at 0.05 %/sec (Fig. 1C). A two-way ANOVA revealed no significant differences ($p > 0.19$) in compressive strength and failure strain between load bearing (n = 8) and non-load bearing articular cartilage explants (n = 8), therefore the combined results (two explants from eight biologically distinct animals per strain rate group) are presented.

3.2. Fatigue and endurance

Articular cartilage explants demonstrated classical fatigue behavior: loading cycles to failure decreased as the magnitude of cyclic stress increased (Fig. 2A). All explants loaded at ≥50 %*S* failed in less than 14,000 cycles. The intermediate loading level 39 %*S* was tested on both the endurometer and MTS 858. For both systems, three explants were cyclically loaded to run-out, while the remaining five failed. All cartilage explants loaded at 10 and 20 %*S* endured 100,000 cycles. A logarithmic curve was fit to the failed explant data set ($\%S = -3.89 \cdot \ln(N) + 76.91,\ R^2 = 0.36,\ p < 9 \times 10^{-6}$), and is consistent with conventional fatigue behavior. Tissue failure, observed as disruption of the bulk tissue, in general led to a sudden acceleration of the peak displacement as typified by a sigmoidal curve (Fig. 2B).

3.3. Equilibrium compressive moduli

The equilibrium compressive moduli of articular cartilage explants were statistically similar ($p > 0.62$) among all loading levels prior to endurance testing (Fig. 3A), with an overall mean of 1.13 ± 0.38 MPa. At the conclusion of endurance testing (Fig. 3B), no differences in equilibrium moduli were observed between run-out samples and unloaded explants (0 %*S*) ($p > 0.61$). However, testing resulted in the pooled equilibrium modulus increasing to 1.59 ± 0.48 MPa ($p < 6 \times 10^{-7}$). The intermediate loading levels of 30 and 39 %*S* had a blend of failures and run-outs, motivating a comparison of the pre-test equilibrium moduli for these samples (Fig. 3C). No significant, prior differences between these groups of explants were detected ($p = 0.08$).

3.4. Explant height recovery and peak strain

Run-out samples at the loading levels of 10, 20, 30, and 39 %*S* recovered 98.7 ± 1.5, 95.8 ± 4.0, 96.9 ± 1.8, and 96.7 ± 2.7 % of their original thicknesses, respectively, compared to 102.3 ± 2.3 % for unloaded controls. The height recovery of run-out explants from loading levels of 20, 30, and 39 %*S* was significantly lower ($p < 0.05$) than unloaded controls. Peak strain was compiled for each loading level at the cycle prior to run-out or failure (Fig. 5A), increasing to a maximum of 78.56 ± 8.54 and 81.91 ± 5.68 % for the loading levels of 39 and 50 %*S*, respectively. At loading levels exceeding 50 %*S*, peak strain trended lower, reaching a significantly lower strain of 66.17 ± 17.31 % at 80 %*S*.

3.5. Fatigue failure analysis

Explants cyclically loaded to failure during endurance testing were characterized to gain a better understanding of potential failure mechanisms (Fig. 4). Failures were classified as either intermediate (Fig. 4C–H) or catastrophic (Fig. 4I–P). Intermediate failures consisted of superficial (Fig. 4C–D) and partial thickness fissures (Fig. 4E–H), whereas catastrophic failure included full-thickness fissures (Fig. 4I–J), ruptures (Fig. 4K–L), and bulk tissue failures (Fig. 4M–P). The peak-to-peak strains for the cycle preceding run-out, intermediate, or failure were significantly different ($p < 0.012$) at 0.83 ± 0.64, 3.96 ± 2.52, and 8.08 ± 5.46 %, respectively (Fig. 5B). These results were inversely related to cycles to failure or run-out (Fig. 5C), where catastrophic failure explants completed significantly fewer cycles (897 ± 3527, median = 41), followed by intermediate failures (4134 ± 4503, median = 2829), and finally run-out samples (100,000 ± 0, $p < 0.004$).

3.6. Histology and biochemical analysis

Histological staining did not reveal any observable differences in collagen and sGAG composition between unloaded control, failure, or run-out samples (Fig. 6). Biochemical analysis corroborated the histology results. No significant differences in collagen ($p > 0.54$), sGAG ($p > 0.48$), and hydration ($p > 0.15$) were observed between unloaded controls and run-out samples (Fig. 7). The

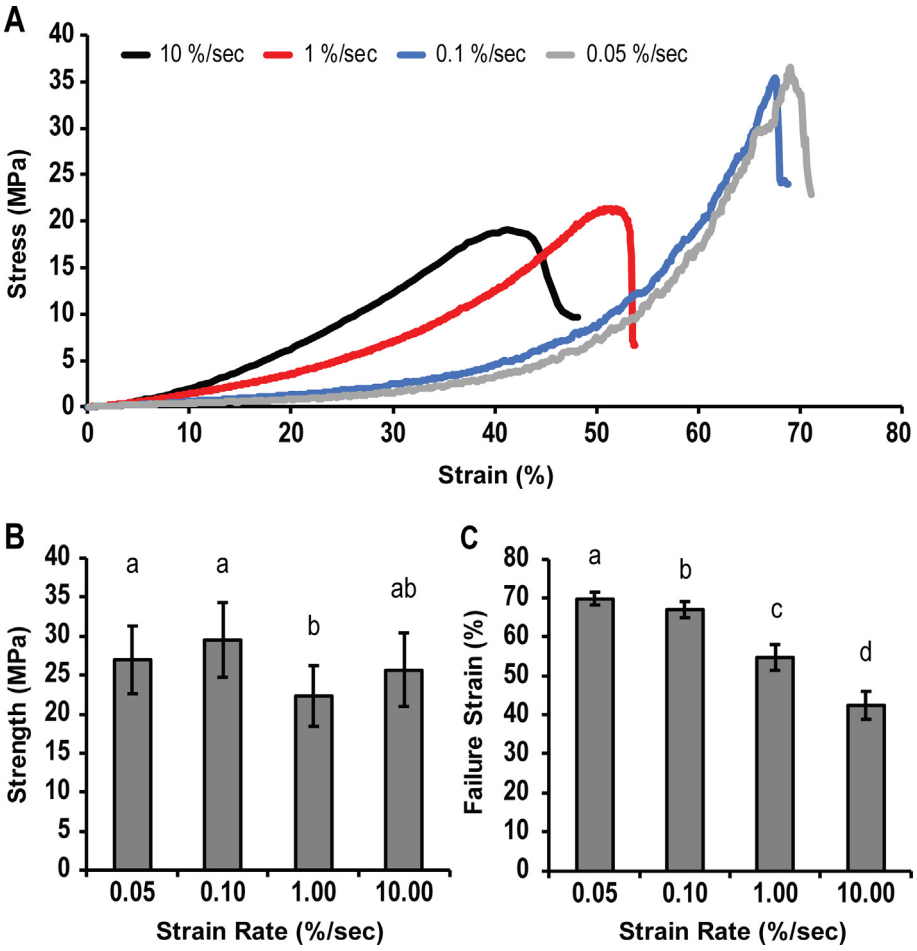

Fig. 1. (A) Representative plot of the stress-strain behavior of juvenile bovine articular cartilage explants (one load bearing and one non-loading bearing explant from eight biologically distinct animals) compressed under strain-rates of 0.05, 0.1, 1, and 10 %/sec. (B) The compressive strength of juvenile cartilage explants is strain rate-dependent, with strengths of 29.5 ± 4.8 MPa and 26.9 ± 4.3 MPa observed at 0.10 %/sec and 0.05 %/sec, respectively. (C) Failure strain increased as the strain rate decreased, with a maximum failure strain of 69.8 ± 1.8 % at 0.05 %/sec. No significant differences ($p > 0.19$) in compressive strength and failure strain between load bearing ($n = 8$) and non-load bearing articular cartilage explants ($n = 8$) were observed via a two-way ANOVA, thus the combined results (two explants from eight biologically distinct animals for every strain rate group) are shown.

respective pooled means, as percentage of wet weight, were 15.4 ± 1.8, 6.0 ± 0.6, and 74.8 ± 2.6 %.

4. Discussion

Fatigue and endurance are remarkably understudied concepts in articular cartilage. Although healthy cartilage can endure millions of cycles of loading *in vivo*, conventional biomechanical and tribological tests replicate only a brief snapshot of this duty cycle. These tests do not impart the repeated stresses that can weaken and fatigue a material over time, leading to break down and functional failure. It is unknown how articular cartilage fatigues under compressive loading, and whether a limiting value of stress exists under which cartilage can support a lifetime of loading (e.g. fatigue or endurance limit). Therefore, the objective of this investigation was to characterize the compressive strength and endurance of articular cartilage. Classical fatigue behavior in juvenile, bovine articular cartilage explants confirmed our hypothesis (Fig. 2A). Histological (Fig. 6) and biochemical analyses (Fig. 7) revealed no significant differences between run-out samples and unloaded controls. This investigation is the first to describe the fatigue life (e.g. S-N or Wöhler curve) of articular cartilage under compressive loading, with an incipient endurance limit of 20 %*S* (5.86 MPa). These results establish a reference for articular cartilage endurance based on native tissue values, and present a method of testing for mechanical durability *in vitro* through endurance testing.

As a biphasic material with time-dependent poroelastic behavior (Wahlquist et al., 2017), the compressive strength of articular cartilage was measured as a function of strain rate (Fig. 1A). Failure strain increased as the strain rate decreased (Fig. 1C). Load support shifts from the fluid phase to the ECM (e.g. solid phase) as the strain rate decreases since lower rates allow for additional fluid loss. Conversely, interstitial fluid pressurization increases as the strain rate increases (Torzilli et al., 1983), imposing additional stress on the ECM that leads to tissue failure at lower strains (Morel and Quinn, 2004). Compressive strength varied non-linearly with respect to strain rate as the compressive strength observed at 10 %/sec was intermediate of the strength values recorded at 1 and 0.1 %/sec (Fig. 1B). This response is another demonstration of stress-strain non-linearities that arise from the biphasic nature of this tissue, and presents another parameter that can be utilized to improve constitutive models of articular cartilage biomechanics (Mow et al., 1992).

There was no significant difference in compressive strength between articular cartilage obtained from load bearing and non-load bearing regions of the medial, femoral condyle. While this similarity might be due to the relative immaturity of juvenile articular cartilage, our results are comparable to a report by Kerin and

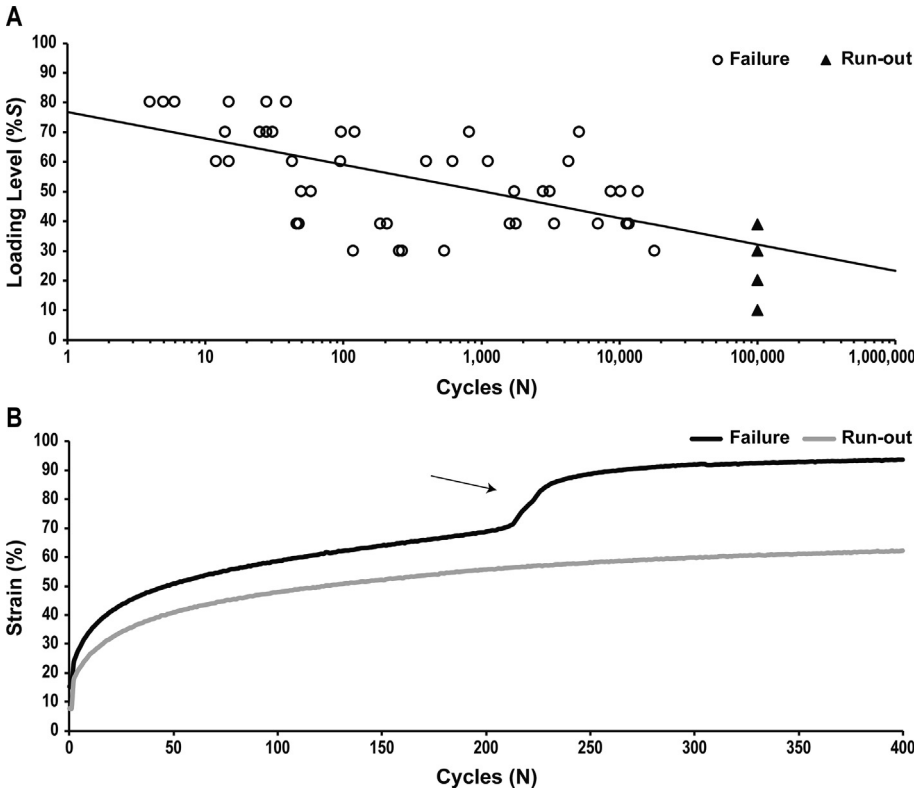

Fig. 2. (A) Fatigue life (e.g. S-N or Wöhler curve) of juvenile, bovine articular cartilage explants at loading levels ranging from 10 to 80 %*S* (○ Failure, ▲ Run-out). At low loading levels of 10 to 20 %*S*, all explants were cyclically loaded to run-out at 100,000 cycles. Explants at the highest loading levels, 50 to 80 %*S*, all failed. In the intermediate loading levels of 30 to 39 %*S*, a blend of failures and run-outs was observed. A logarithmic curve (solid line) was fit to the failure sample data set ($\%S = -3.89 \cdot \ln(N) + 76.91$, $R^2 = 0.36$, $p < 9 \times 10^{-6}$). (B) A representative plot of the cyclic peak strain values of an articular cartilage explant during failure, compared with an explant that was loaded to run-out. This sigmoidal characteristic (arrow) in cyclic peak strain curve was observed to be indicative of compressive failure in response to cyclic loading of articular cartilage explants.

colleagues (1998) who reported the compressive strength of mature, bovine articular cartilage as 35.7 ± 11.0 MPa. Similarly, no significant differences in equilibrium confined compressive modulus and collagen content were observed between juvenile and adult bovine articular cartilage (Williamson et al., 2001). The collagen network is likely an important determinant of articular cartilage strength due to its role in counterbalancing interstitial fluid pressure via tension–compression non-linearity (Ateshian, 2009).

Juvenile articular cartilage displays classical fatigue behavior (Fig. 2A). Cycles to failure increased as the loading level decreased. At loading levels of 10 and 20 %*S*, all articular cartilage explant samples ran-out, withstanding 10^5 loading cycles. This result is similar to a report by Zimmerman and colleagues (1988) where human patellar cartilage was undamaged after 120,860 cycles of compression at 3.49 MPa. Equilibrium compressive moduli were similar between all explants prior to testing (Fig. 3A), and between unloaded controls and run-out samples (Fig. 3B). Likewise, hydration, collagen, and sGAG content (Figs. 6 and 7) were similar between unloaded controls and run-out samples, with levels falling within native tissue levels (Mow et al., 1992). This maintenance of sGAG content in articular cartilage explants subjected to cyclic loading was previously noted by Torzilli and Grigiene (1998). While typically measured after 10^6–10^7 cycles, this preliminary evidence suggests an endurance limit for articular cartilage may exist. Interestingly, an endurance limit of 20 %*S* (5.86 MPa) aligns with the range of contact stresses (1–6 MPa) articular cartilage experiences during routine activities (Brand, 2005; Park et al., 2004). Although additional work is needed to verify this incipient endurance limit extends to 10^7 cycles in both juvenile and adult articular cartilage, an alignment between endurance strength and anabolic, physiological contact stresses would fit within a structure-function framework. Loading magnitudes that elicit catabolic cellular responses may have other detrimental effects such as a reduction in endurance.

This investigation developed a novel, objective assessment of mechanical failure during cyclic, compressive loading through peak strain analysis. Of note, repetitive loading resulted in failure modes (Fig. 4C–J) that resemble OA chondral lesions, such as fissures and stellate fractures (Bauer and Jackson, 1988; Falah et al., 2010). However, the role of mechanical fatigue in OA pathogenesis remains an open question. Additionally, the continuous cyclic loading required for this endurance testing approach resulted in supraphysiological strains on articular cartilage explants that spanned between 60.04 ± 4.66 % and 81.91 ± 5.68 % (Fig. 5A). For reference, *in vivo* tibiofemoral cartilage strains range between 2 and 23 % in response to ADL (Coleman et al., 2013; Liu et al., 2010). While the loading frequency employed falls within *in vivo* physiological rates (Waters et al., 1988), dynamic creep lead to the loss of interstitial fluid and accompanying load support. Thus, the fatigue and endurance behavior observed is likely representative of the solid phase or ECM of articular cartilage. It is important to note that run-out explants recovered between 95.8 ± 4.0 and 98.7 ± 1.5 % of their thickness following endurance testing, demonstrating the ability to rehydrate and regain interstitial fluid. While interstitial fluid pressurization is a critical aspect of articular cartilage that buffers and reduces stresses on the ECM (Ateshian, 2009), an understanding of the endurance properties of the solid phase is critical to a better understanding of articular cartilage mechanical behavior and performance.

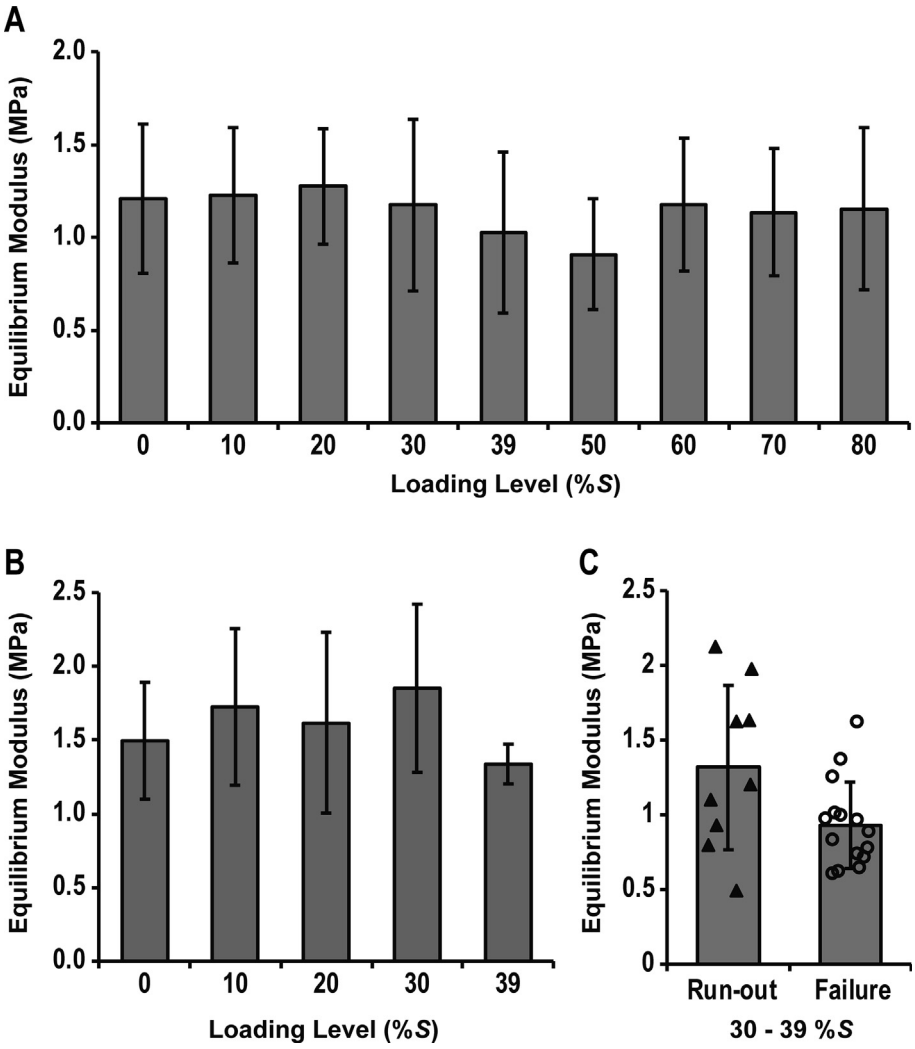

Fig. 3. (A) Equilibrium moduli of articular cartilage explants, prior to the commencement of endurance testing, showed no significant differences ($p > 0.62$) across all loading levels (0 to 80 %*S*). (B) At the conclusion of endurance testing, no significant differences in equilibrium moduli were observed ($p > 0.62$) between unloaded explants (0 %*S*) and fatigued explants cyclically loaded to run-out. (C) At the loading levels of 30 and 39 %*S*, where there was a mixture of failed and run-out explants, a *post hoc* analysis did not reveal any differences ($p = 0.08$) in equilibrium modulus between these two subgroups prior to endurance testing.

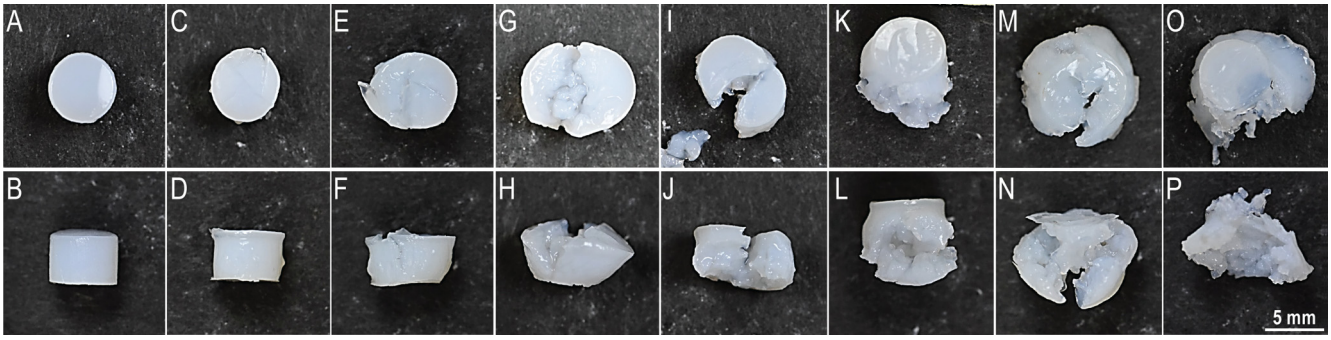

Fig. 4. Articular cartilage explants failed along several anatomical planes during endurance testing. Unloaded articular cartilage explants (A, B) and tissues fatigued to failure during endurance testing (C–P) are shown (top: transverse view; bottom: sagittal view). Failures were classified as intermediate (C–H) and catastrophic (I–P). Intermediate failures were composed of superficial (C, D) and partial thickness fissures (E–H) through a plane perpendicular to the articular surface. Catastrophic failures included full-thickness fissures (I, J), ruptures along a plane parallel to the articular surface (K, L), and bulk tissue failures (M–P).

Much remains unknown regarding articular cartilage endurance. At the top of this list are the key structure-function relationships that support healthy articular cartilage that withstands a lifetime of activity. For example, collagen network modifications mediated by pyridinoline cross-links or small leucine-rich proteoglycans such as decorin may play a role (Eyre, 2004; Melrose et al., 2008). An additional unknown parameter is the effect of cellular metabolism on extracellular matrix development and remodeling.

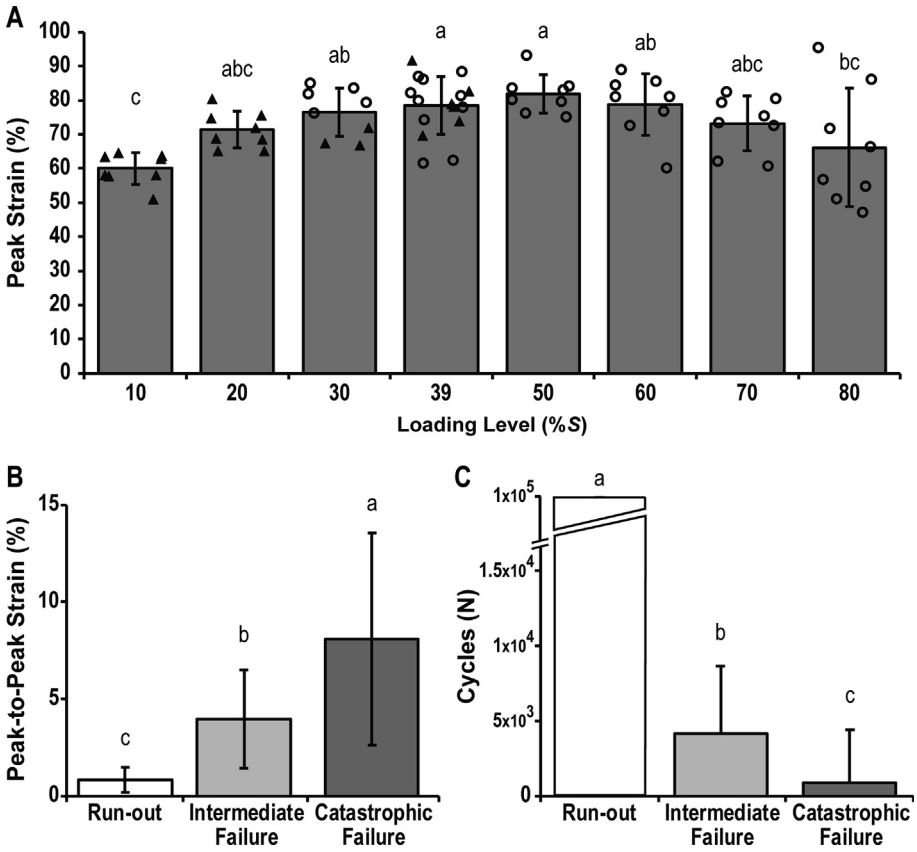

Fig. 5. (A) Peak strain of articular cartilage explants varied between loading levels (Failure ○, Run-out ▲), reaching a maximum strain of 78.56 ± 8.54 % at 39 %*S*, and 81.91 ± 5.68 % at 50 %*S*. (B) Peak-to-peak strain of the loading cycle prior to run-out, intermediate failure, and catastrophic failure significantly differed between each event, respectively measured at 0.83 ± 0.64, 3.96 ± 2.52, and 8.08 ± 5.46 %. Catastrophic failures corresponded to the greatest strain rate during the final loading cycle, while run-outs had the lowest values ($p < 0.012$). (C) In comparison, cycles to run-out, intermediate failure, and catastrophic failure had the opposite trend as explants loaded to catastrophic failure supported fewer loading cycles than explants tested to intermediate failure and run-out ($p < 0.004$).

Over the last few decades, articular cartilage mechanotransduction studies have identified mechanical loading regimens that result in anabolic increases in sGAG and collagen synthesis (Palmoski and Brandt, 1984; Sah et al., 1989), as well as catabolic responses to mechanical stimuli (Guilak et al., 1994; Thibault et al., 2002; Li et al., 2013). For the purposes of this introductory investigation into articular cartilage endurance, articular cartilage explants devitalized by freezing were utilized to avoid confounding effects from cellular responses to the endurance testing protocol. The accelerated nature of the endurance testing protocol also precluded the incorporation of periods of inactivity that occur during rest and sleep. Futures investigations into articular cartilage endurance should take into consideration the effects of species (i.e. human), loading frequency, magnitude, duration, and duty cycle on articular chondrocyte metabolism, resultant tissue remodeling, and overall mechanical endurance on articular cartilage.

To more fully recapitulate the biomechanical loading environment, future studies of endurance should include articular cartilage articulation/sliding. Inclusion of this loading modality through models such as migrating contact area (MCA) or stationary contact area sliding with tribological rehydration would also better reflect the maintenance of interstitial fluid pressurization observed *in vivo* (Caligaris and Ateshian, 2008; Graham et al., 2018). MCA and tribological rehydration are complementary models of physiological loading that seek to preserve interstitial fluid pressure for articular cartilage biomechanics and lubrication. In contrast to conventional biomechanical models that continuously load the surface of a cartilage explant, MCA recapitulates the shifting contact area observed during tibiofemoral joint articulation (Caligaris and Ateshian, 2008). Relatedly, tribological rehydration suggests physiological sliding speeds of 60 mm/s are critical to promote fluid recovery and thus maintenance of interstitial fluid pressurization (Graham et al., 2018). These loading regimens would improve the physiological fidelity of endurance testing through maintenance of interstitial fluid pressurization, as well as capture the effects of tribological loading and wear from articular cartilage sliding.

Endurance testing presents the opportunity to examine biomechanical durability *in vitro*, an assay relevant for the functional tissue engineering of articular cartilage (Guilak et al., 2014). Current durability tests rely on animal models (U.S. Food and Drug Administration, 2011). While endurance testing won't replace *in vivo* models, which offer additional information such as maturation in a biological milieu, endurance testing characterizes biomechanical robustness, a parameter not captured by typical monotonic tests. The field is beginning to move in this direction with the incorporation of compressive failure testing (Beck et al., 2016; Cigan et al., 2016). To advance progress in this discipline and reduce the reliance on animal models, articular cartilage tissue engineering should begin to develop new methods that capture *in vitro* mechanical durability over a period of time, such as the endurance testing approach described here.

Acknowledgements

The authors wish to thank Drs. A. Hari Reddi, Kyriacos Athanasiou, Jerry Hu, and Richard A. Marder for their discussions and support. This investigation was supported in part by the Lawrence J. Ellison Chair in Musculoskeletal Molecular Biology at the University of California, Davis.

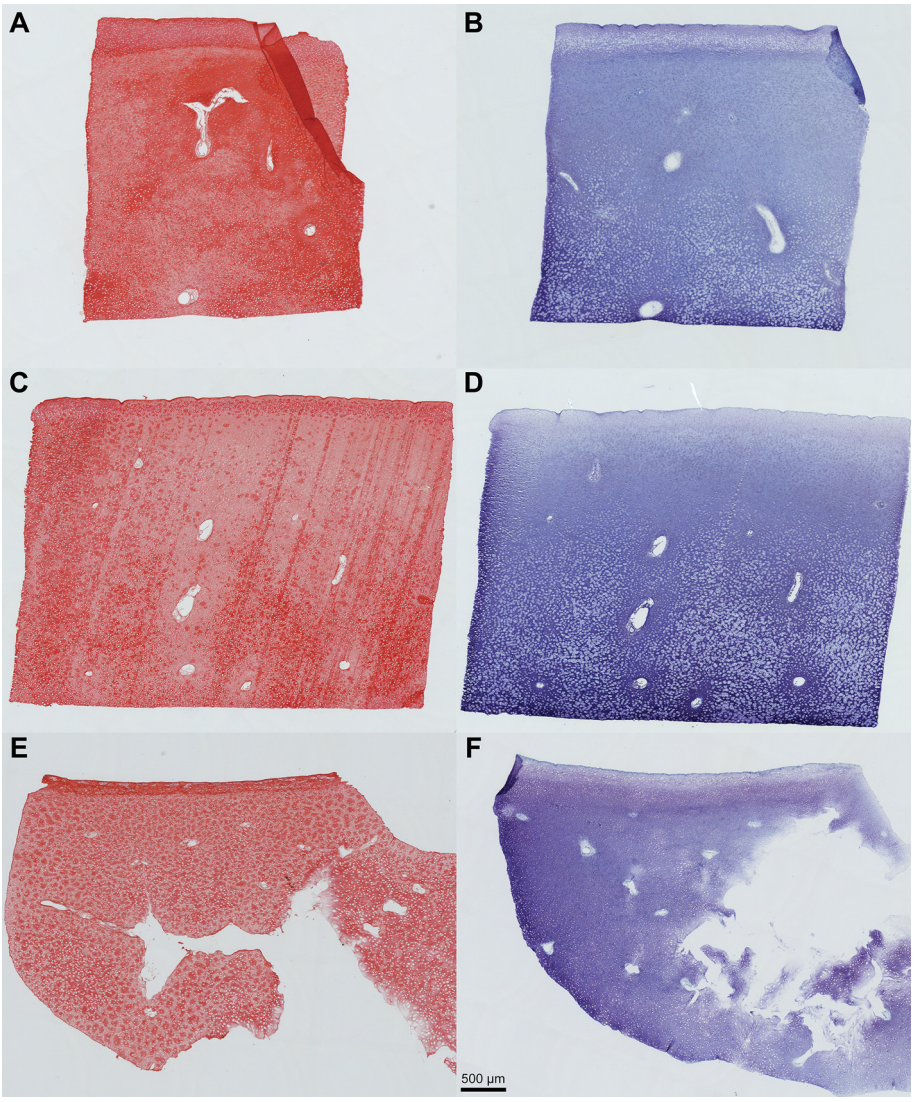

Fig. 6. Histological sections of an unloaded articular cartilage explant (A, B), run-out explant following 100,000 loading cycles at 20 %*S* (C, D), and explant cyclically loaded to failure from the 30 %*S* loading level (E, F) are presented. Picrosirius red staining of collagen was similar between unloaded (A), run-out (C), and failed explants (E). Likewise, toluidine blue staining demonstrates similar sulfated glycosaminoglycan content between explants from these treatment groups (scale bar: 500 µm). (For interpretation of the references to colour in this figure legend, the reader is referred to the web version of this article.)

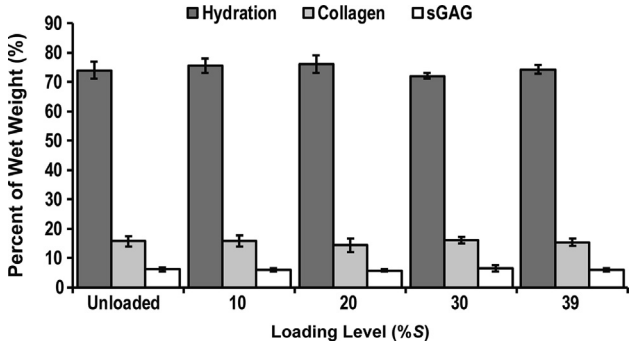

Fig. 7. Hydration, collagen content, and sulfated glycosaminoglycan (sGAG) content of unloaded articular cartilage explants, and tissues cyclically loaded to run-out after 100,000 cycles of endurance testing at 10, 20, 30, and 39 %*S* were normalized to wet weight. No significant differences were detected between the loading levels with respect to hydration ($p > 0.15$), collagen ($p > 0.54$), and sGAG ($p > 0.48$) content.

Declaration of Competing Interest

The authors affirm that there are no conflicts of interest.

Appendix A. Supplementary material

Supplementary data to this article can be found online at https://doi.org/10.1016/j.jbiomech.2019.07.048.

References

Ateshian, G.A., 2009. The role of interstitial fluid pressurization in articular cartilage lubrication. J. Biomech. 42, 1163–1176.
Athanasiou, K.A., Rosenwasser, M.P., Buckwalter, J.A., Malinin, T.I., Mow, V.C., 1991. Interspecies comparisons of in situ intrinsic mechanical properties of distal femoral cartilage. J. Orthop. Res. 9, 330–340.
Bauer, M., Jackson, R.W., 1988. Chondral lesions of the femoral condyles: a system of arthroscopic classification. Arthrosc.: J. Arthrosc. Relat. Surg. 4, 97–102.

Beck, E.C., Barragan, M., Tadros, M.H., Gehrke, S.H., Detamore, M.S., 2016. Approaching the compressive modulus of articular cartilage with a decellularized cartilage-based hydrogel. Acta Biomater. 38, 94–105.
Bellucci, G., Seedhom, B.B., 2002. Tensile fatigue behaviour of articular cartilage. Biorheology 39, 193–199.
Brand, R.A., 2005. Joint contact stress: a reasonable surrogate for biological processes? Iowa Orthop. J. 25, 82–94.
Caligaris, M., Ateshian, G.A., 2008. Effects of sustained interstitial fluid pressurization under migrating contact area, and boundary lubrication by synovial fluid, on cartilage friction. Osteoarthrit. Cartil. 16, 1220–1227.
Canal, C.E., Hung, C.T., Ateshian, G.A., 2008. Two-dimensional strain fields on the cross-section of the bovine humeral head under contact loading. J. Biomech. 41, 3145–3151.
Chan, D.D., Cai, L., Butz, K.D., Trippel, S.B., Nauman, E.A., Neu, C.P., 2016. In vivo articular cartilage deformation: noninvasive quantification of intratissue strain during joint contact in the human knee. Sci. Rep. 6, 19220.
Chapra, S., Canale, R., 2015. Truncation Errors and the Taylor Series. In: Numerical Methods for Engineers. seventh ed. McGraw-Hill, New York, pp. 81–109.
Cigan, A.D., Durney, K.M., Nims, R.J., Vunjak-Novakovic, G., Hung, C.T., Ateshian, G. A., 2016. Nutrient channels aid the growth of articular surface-sized engineered cartilage constructs. Tissue Eng. Part A 22, 1063–1074.
Cissell, D.D., Link, J.M., Hu, J.C., Athanasiou, K.A., 2017. A modified hydroxyproline assay based on hydrochloric acid in Ehrlich's solution accurately measures tissue collagen content. Tissue Eng. Part C Methods 23, 243–250.
Coleman, J.L., Widmyer, M.R., Leddy, H.A., Utturkar, G.M., Spritzer, C.E., Moorman, C. T., Guilak, F., DeFrate, L.E., 2013. Diurnal variations in articular cartilage thickness and strain in the human knee. J. Biomech. 46, 541–547.
Eyre, D.R., 2004. Collagens and cartilage matrix homeostasis. Clin. Orthop. Relat. Res., S118–S122
Falah, M., Nierenberg, G., Soudry, M., Hayden, M., Volpin, G., 2010. Treatment of articular cartilage lesions of the knee. Int. Orthop. 34, 621–630.
Felson, D.T., 2013. Osteoarthritis as a disease of mechanics. Osteoarthrit. Cartil. 21, 10–15.
Graham, B.T., Moore, A.C., Burris, D.L., Price, C., 2018. Mapping the spatiotemporal evolution of solute transport in articular cartilage explants reveals how cartilage recovers fluid within the contact area during sliding. J. Biomech. 71, 271–276.
Guilak, F., Butler, D.L., Goldstein, S.A., Baaijens, F.P., 2014. Biomechanics and mechanobiology in functional tissue engineering. J. Biomech. 47, 1933–1940.
Guilak, F., Meyer, B.C., Ratcliffe, A., Mow, V.C., 1994. The effects of matrix compression on proteoglycan metabolism in articular cartilage explants. Osteoarthrit. Cartil. 2, 91–101.
Hodge, W.A., Fijan, R.S., Carlson, K.L., Burgess, R.G., Harris, W.H., Mann, R.W., 1986. Contact pressures in the human hip joint measured in vivo. Proc. National Acad. Sci. U.S.A. 83, 2879–2883.
Kaplan, J.T., Neu, C.P., Drissi, H., Emery, N.C., Pierce, D.M., 2017. Cyclic loading of human articular cartilage: The transition from compaction to fatigue. J. Mech. Behav. Biomed. Mater. 65, 734–742.
Kerin, A.J., Wisnom, M.R., Adams, M.A., 1998. The compressive strength of articular cartilage. Proc. Inst. Mech. Eng. Part H: J. Eng. Med. 212, 273–280.
Ko, F.C., Dragomir, C., Plumb, D.A., Goldring, S.R., Wright, T.M., Goldring, M.B., van der Meulen, M.C., 2013. In vivo cyclic compression causes cartilage degeneration and subchondral bone changes in mouse tibiae. Arthritis Rheum. 65, 1569–1578.
Lapvetelainen, T., Nevalainen, T., Parkkinen, J.J., Arokoski, J., Kiraly, K., Hyttinen, M., Halonen, P., Helminen, H.J., 1995. Lifelong moderate running training increases the incidence and severity of osteoarthritis in the knee joint of C57BL mice. Anat. Rec. 242, 159–165.
Li, Y., Frank, E.H., Wang, Y., Chubinskaya, S., Huang, H.H., Grodzinsky, A.J., 2013. Moderate dynamic compression inhibits pro-catabolic response of cartilage to mechanical injury, tumor necrosis factor-alpha and interleukin-6, but accentuates degradation above a strain threshold. Osteoarthrit. Cartil. 21, 1933–1941.
Liu, F., Kozanek, M., Hosseini, A., Van de Velde, S.K., Gill, T.J., Rubash, H.E., Li, G., 2010. In vivo tibiofemoral cartilage deformation during the stance phase of gait. J. Biomech. 43, 658–665.
Mauck, R.L., Soltz, M.A., Wang, C.C.B., Wong, D.D., Chao, P.-H.G., Valhmu, W.B., Hung, C.T., Ateshian, G.A., 2000. Functional tissue engineering of articular cartilage through dynamic loading of chondrocyte-seeded agarose gels. J. Biomech. Eng. 122, 252–260.
McCormack, T., Mansour, J.M., 1998. Reduction in tensile strength of cartilage precedes surface damage under repeated compressive loading in vitro. J. Biomech. 31, 55–61.
McNary, S.M., Athanasiou, K.A., Reddi, A.H., 2012. Engineering lubrication in articular cartilage. Tissue Eng. Part B Rev. 18, 88–100.
Melrose, J., Fuller, E.S., Roughley, P.J., Smith, M.M., Kerr, B., Hughes, C.E., Caterson, B., Little, C.B., 2008. Fragmentation of decorin, biglycan, lumican and keratocan is elevated in degenerate human meniscus, knee and hip articular cartilages compared with age-matched macroscopically normal and control tissues. Arthrit. Res. Therapy 10, R79.
Morel, V., Quinn, T.M., 2004. Cartilage injury by ramp compression near the gel diffusion rate. J. Orthop. Res. 22, 145–151.
Mow, V.C., Gibbs, M.C., Lai, W.M., Zhu, W.B., Athanasiou, K.A., 1989. Biphasic indentation of articular cartilage–II. A numerical algorithm and an experimental study. J. Biomech. 22, 853–861.
Mow, V.C., Ratcliffe, A., Poole, A.R., 1992. Cartilage and diarthrodial joints as paradigms for hierarchical materials and structures. Biomaterials 13, 67–97.
Neu, C.P., Khalafi, A., Komvopoulos, K., Schmid, T.M., Reddi, A.H., 2007. Mechanotransduction of bovine articular cartilage superficial zone protein by transforming growth factor beta signaling. Arthrit. Rheum. 56, 3706–3714.
Palmoski, M.J., Brandt, K.D., 1984. Effects of static and cyclic compressive loading on articular cartilage plugs in vitro. Arthrit. Rheum. 27, 675–681.
Park, S., Hung, C.T., Ateshian, G.A., 2004. Mechanical response of bovine articular cartilage under dynamic unconfined compression loading at physiological stress levels. Osteoarthrit. Cartil. 12, 65–73.
Park, S., Krishnan, R., Nicoll, S.B., Ateshian, G.A., 2003. Cartilage interstitial fluid load support in unconfined compression. J. Biomech. 36, 1785–1796.
Peng, G., McNary, S.M., Athanasiou, K.A., Reddi, A.H., 2014. Surface zone articular chondrocytes modulate the bulk and surface mechanical properties of the tissue-engineered cartilage. Tissue Eng. Part A 20, 3332–3341.
Peng, G., McNary, S.M., Athanasiou, K.A., Reddi, A.H., 2015. The distribution of superficial zone protein (SZP)/lubricin/PRG4 and boundary mode frictional properties of the bovine diarthrodial joint. J. Biomech. 48, 3406–3412.
Poulet, B., Hamilton, R.W., Shefelbine, S., Pitsillides, A.A., 2011. Characterizing a novel and adjustable noninvasive murine joint loading model. Arthrit. Rheum. 63, 137–147.
Radin, E.L., Martin, R.B., Burr, D.B., Caterson, B., Boyd, R.D., Goodwin, C., 1984. Effects of mechanical loading on the tissues of the rabbit knee. J. Orthop. Res. 2, 221–234.
Sadeghi, H., Espino, D.M., Shepherd, D.E., 2017. Fatigue strength of bovine articular cartilage-on-bone under three-point bending: the effect of loading frequency. BMC Musculoskelet. Disord. 18, 142.
Sadeghi, H., Lawless, B.M., Espino, D.M., Shepherd, D.E.T., 2018. Effect of frequency on crack growth in articular cartilage. J. Mech. Behav. Biomed. Mater. 77, 40–46.
Sadeghi, H., Shepherd, D.E., Espino, D.M., 2015. Effect of the variation of loading frequency on surface failure of bovine articular cartilage. Osteoarthrit. Cartil. 23, 2252–2258.
Sah, R.L., Kim, Y.J., Doong, J.Y., Grodzinsky, A.J., Plaas, A.H., Sandy, J.D., 1989. Biosynthetic response of cartilage explants to dynamic compression. J. Orthop. Res. 7, 619–636.
Sandell, L.J., 2012. Etiology of osteoarthritis: genetics and synovial joint development. Nat. Rev. Rheumatol. 8, 77–89.
Simon, S.R., Radin, E.L., Paul, I.L., Rose, R.M., 1972. The response of joints to impact loading. II. In vivo behavior of subchondral bone. J. Biomech. 5, 267–272.
Simon, W.H., Mak, A., Spirt, A., 1989. The effect of shear fatigue on bovine articular cartilage. J. Orthop. Res. 8, 86–93.
Suresh, S., 1998. In: Fatigue of Materials. Cambridge University Press, New York, pp. 1–36.
Szarko, M., Muldrew, K., Bertram, J.E., 2010. Freeze-thaw treatment effects on the dynamic mechanical properties of articular cartilage. BMC Musculoskelet. Disord., 11
Thibault, M., Robin Poole, A., Buschmann, M.D., 2002. Cyclic compression of cartilage/bone explants in vitro leads to physical weakening, mechanical breakdown of collagen and release of matrix fragments. J. Orthop. Res. 20, 1265–1273.
Torzilli, P.A., Dethmers, D.A., Rose, D.E., Schryuer, H.F., 1983. Movement of interstitial water through loaded articular cartilage. J. Biomech. 16, 169–179.
Torzilli, P.A., Grigiene, R., 1998. Continuous cyclic load reduces proteoglycan release from articular cartilage. Osteoarthrit. Cartil. 6, 260–268.
Tudor-Locke, C., Hart, T.L., Washington, T.L., 2009. Expected values for pedometer-determined physical activity in older populations. Int. J. Behav. Nutrit. Phys. Act. 6, 59.
U.S. Food and Drug Administration, 2011. Guidance for Industry: Preparation of IDEs and INDs for Products Intended to Repair or Replace Knee Cartilage, http://www.fda.gov/downloads/BiologicsBloodVaccines/GuidanceComplianceRegulatoryInformation/Guidances/CellularandGeneTherapy/UCM288011.pdf.
Wahlquist, J.A., DelRio, F.W., Randolph, M.A., Aziz, A.H., Heveran, C.M., Bryant, S.J., Neu, C.P., Ferguson, V.L., 2017. Indentation mapping revealed poroelastic, but not viscoelastic, properties spanning native zonal articular cartilage. Acta Biomater. 64, 41–49.
Waters, R.L., Lunsford, B.R., Perry, J., Byrd, R., 1988. Energy-speed relationship of walking: standard tables. J. Orthop. Res. 6, 215–222.
Weightman, B., Chappell, D.J., Jenkins, E.A., 1978. A second study of tensile fatigue properties of human articular cartilage. Ann. Rheum. Dis. 37, 58–63.
Weightman, B.O., Freeman, M.A., Swanson, S.A., 1973. Fatigue of articular cartilage. Nature 244, 303–304.
Williamson, A.K., Chen, A.C., Sah, R.L., 2001. Compressive properties and function-composition relationships of developing bovine articular cartilage. J. Orthop. Res. 19, 1113–1121.
Zimmerman, N.B., Smith, D.G., Pottenger, L.A., Cooperman, D.R., 1988. Mechanical disruption of human patellar cartilage by repetitive loading in vitro. Clin. Orthop. Relat. Res., 302–307